Vol. 11(3): 408-426, September 2023 DOI: https://doi.org/10.23960/jsl.v11i3.761

Jurnal Sylva Lestari

P-ISSN: 2339-0913
E-ISSN: 2549-5747

Journal homepage: https://sylvalestari.fp.unila.ac.id

Full Length Research Article

The Physical and Magnetic Properties of Sengon (*Falcataria moluccana*) Wood Impregnated with Synthesized Magnetite Nanoparticles

Saviska Luqyana Fadia[1], Istie Sekartining Rahayu[*2], Deded Sarip Nawawi[2], Rohmat Ismail[3], Esti Prihatini[2]

[1] Master Study Program in Forest Products Science and Technology, Graduate School, IPB University, Bogor, Indonesia
[2] Department of Forest Products, Faculty of Forestry and Environment, IPB University, Bogor, Indonesia
[3] Department of Chemistry, Faculty of Mathematics and Natural Sciences, IPB University, Bogor, Indonesia
[*] Corresponding Author. E-mail address: istiesr@apps.ipb.ac.id

ARTICLE HISTORY:

Received: 12 July 2023
Peer review completed: 22 July 2023
Received in revised form: 4 August 2023
Accepted: 22 August 2023

KEYWORDS:

Impregnation
Magnetite nanoparticles
Magnetic properties
Physical properties
Sengon

ABSTRACT

Sengon (*Falcataria moluccana*) is one of the fast-growing wood that dominates Indonesian plantation forests. The qualities and utilizations of sengon wood need to be improved and enlarged using magnetite nanoparticles. The research aims to examine the effects on the physical and magnetic properties of sengon wood after being treated by magnetite nanoparticle impregnation. Magnetite nanoparticles were prepared by co-precipitation method with a precursor solution of iron ions mixture and weak base (NH_4OH). The treatments comprised untreated, 1%, and 5% magnetite nanoparticles. Weight percentage gain (WPG), bulking effect (BE), anti-swelling efficiency (ASE), and density tended to increase along with the increase in concentration. Analysis of variance showed that treatment significantly affected WPG, BE, ASE, and density of treated sengon wood. Scanning electron microscopy and energy-dispersive X-ray spectroscopy analysis showed the existence of Fe deposition in the wood cell membranes. X-ray diffraction analysis observed the appearance of magnetic peaks in the diffractogram with the decrease of crystallinity and the increase in concentration. In addition, Fourier transform infrared spectrometry analysis revealed Fe-O functional groups. Based on the vibrating sample magnetometry study, the sengon magnetic wood is classified as a superparamagnetic material with mild magnetic characteristics.

1. Introduction

Sengon (*Falcataria moluccana*) is one of the rapidly enhancing wood species that has the potential to be raw material in the future that can be harvested at a relatively short age (Krisnawati et al. 2011). Nevertheless, fast-growing wood species generally had low dimensional stabilization (Priadi et al. 2019), low density, and easily attack by insects and fungi (Fajriani et al. 2013). Its utilization is still limited only to plywood, wood packaging, lightweight construction materials, and furniture. Therefore, to improve the quality of sengon wood, it is necessary to provide technologies such as wood modification that can be carried out mechanically, thermally, or chemically to diversify the use of wood (Zelinka et al. 2022). This study used the impregnation method proposed by Hill (2006) to enhance wood quality by adding chemical solutions into the wood to modify wood properties at the cell wall level. Recent studies reported the improvement

of the physical properties of sengon and jabon wood with impregnation method using commercial magnetite and silica nanoparticles (Laksono et al. 2023; Rahayu et al. 2021; Rahayu et al. 2022; Wahyuningtyas et al. 2022). This study is in the early stage of examining the physical and magnetic properties of impregnated sengon wood with synthesized magnetite (Fe_3O_4) nanoparticles and demineralized water as solvent.

Research on wood as a functional material continues to evolve for various purposes, including magnetic wood. Magnetic wood is a combination of wood with magnetite nanoparticles solution that has high dimensional stability, magnetic properties that a magnet can attract, and electromagnetic wave absorbance material (Trey et al. 2014). In addition, magnetic wood is a material that can absorb electromagnetic radiation and heat. The development of wireless-based electronic and communication technology has been growing rapidly. However, it can potentially harm the environment and human health due to electromagnetic radiation (Mashkour and Ranjbar 2018). Magnetic wood could be a functional material that can absorb electromagnetic waves. Magnetic wood can be applied to several products, such as electronic components and communication devices, furniture coatings, interior decorative components, and packaging (Liu et al. 2021; Trey et al. 2014). This study focuses on enlarging the utilization of sengon wood by creating a new function for fast-growing wood, namely magnetic wood, which improved physical and magnetic properties.

The synthesis of magnetic wood can be carried out using *in-situ* (Dong et al. 2015; Rahayu et al. 2022) and *ex-situ* methods (Laksono et al. 2023; Wahyuningtyas et al. 2022). The *ex-situ* method was carried out by synthesis of magnetite nanoparticles by co-precipitation method, then impregnated to sengon wood. Oka and Fujita (1999) successfully synthesized magnetic wood by impregnation, coating, and combining the wood with powder or magnetic solution. Other studies by Dong et al. (2015) and Rahayu et al. (2022) succeeded in synthesizing magnetic wood using the *in-situ* method through chemical precipitation. Making magnetic wood using the *ex-situ* method has the advantage that the size of the nanoparticles can be influenced by the dimensions of the wood because this method forms the magnetite nanoparticles by synthesizing the nanoparticle first and then impregnating them into the wood with several concentrations. Magnetite nanoparticles are one of the nanoparticle materials. The nanometer-sized particles can be well distributed and penetrate wood because of their low viscosity, effectiveness in covering wood surfaces, and high dispersion stability (Fufa and Hovde 2010; Teng et al. 2018). Zhang et al. (2006) stated that the magnetite nanoparticles formed in wood are larger when using NH_4OH as a precipitant than a strong base because NH_4OH is a weak base. Furthermore, Peternele et al. (2014) stated that if compared with a strong base, the synthesized Fe_3O_4 results in a few particles with larger sizes, but it produces higher magnetic properties quality and homogeneity of magnetite particle size.

Demineralized water is generally used as a dispersant because water is a universal solvent and has been treated to remove all metal ions that could react with magnetite nanoparticles (Sutopo 2019). This tendency indicates that there are no new reactions during the synthesis process except for the formation of magnetite nanoparticles. Besides that, its waste does not harm nature and the environment. Therefore, in this study, magnetite nanoparticles were synthesized using demineralized water and NH_4OH as a precursor and impregnated into sengon wood to find the best treatment for improving the quality of the sengon wood.

2. Materials and Methods

2.1. Materials

Sengon (*Falcataria moluccana*) woods were collected from a local forest in Bogor, West Java, Indonesia, at 6° 33' 15.9" S 106° 41' 31.9" E. The trees are six-year-old sengon with the diameter at breast height of 35–40 cm. Defect-free samples with the length of 18–20 cm were cut simultaneously from the same tree at branch-free height without distinguishing sapwood and heartwood because this fast-growing species is dominated by juvenile wood. The chemicals used included Iron (II) chloride tetrahydrate ($FeCl_2$) (EMSURE, Merck, Darmstadt, Germany), Iron (III) chloride hexahydrate ($FeCl_3$) (EMSURE, Merck, Darmstadt, Germany), demineralized water (Trisakti, Bogor, Indonesia), Ethylenediaminetetraacetic acid (EDTA) (Titriplex, Merck, Darmstadt, Germany), Ammonium hydroxide (NH_4OH) (SUPRAPUR, Merck, Darmstadt, Germany).

2.2. Research Procedures

This study was carried out through several procedures, from wood sample preparation, synthesis of magnetite nanoparticles, and impregnation process until evaluation.

2.2.1. Wood samples preparation

Sengon wood was cut into 80 samples with the size of 2 mm × 2 mm × 2 mm (British Standard Institution 1957) using a chain saw and table circular saw. The boards were then pre-heated in an oven at 103 ± 2°C until reaching a steady mass prior to the evaluation of physical properties and dimensional stability of wood testing such as weight percentage gain (WPG), anti-swelling efficiency (ASE), bulking effect (BE), and wood density.

2.2.2. Synthesis of magnetite nanoparticles

The synthesis process was adapted from previous studies (Dong et al. 2015; Laksono et al. 2023; Wahyuningtyas et al. 2022). First, $FeCl_2$ and $FeCl_3$ were mixed and dissolved in 200 mL of demineralized water with a mole ratio of 1:1.6 (Dong et al. 2015) by the co-precipitation method (Peternele et al. 2014). The mixture of Fe solution was then stirred with a magnetic stirrer until homogeneous. EDTA of 0.292 g dissolved in 100 mL of demineralized water was added, and the solution was vacuumed for 15 min. While vacuuming, 40 mL of NH_4OH was prepared by scaling it on the Erlenmeyer flask. The NH_4OH solution was then added through a separating funnel until the color of the solution turned black and reached the pH of 12 to allow magnetite nanoparticles to be formed. The solution was then vacuumed and stirred again for 15 minutes. After the vacuum process was completed, the pH of magnetite nanoparticles was reduced by washing it several times with demineralized water until it reached a pH of 9. The samples were then heated in an oven at 40 °C until formed the magnetite nanoparticles.

2.2.3. Preparation of impregnation solution

Impregnation solutions with various compositions (**Table 1)** were mixed using a sonicator (Ultrasonic) with an amplitude of 40% for 15 minutes. After that, the wood samples were immersed in the impregnation solution.

Table 1. Magnetite nanoparticles (Fe_3O_4) composition with various dispersants composition

No.	Demineralized water (mL)	Magnetite nanoparticles (g)	Treatment (wt %)
1	250	0	0
2	250	2.5	1
3	250	12.5	5

2.2.4. Impregnation Process

The impregnation process was adopted by previous studies (Dong et al. 2015; Oka et al. 2002; Rahayu et al. 2022). The immersed samples with several treatments were then placed into the impregnation tube, followed by a vacuum using the tension of 50% bar for 2 h and continued with a tension of 1 bar for 0.5 h. After impregnation, polymerization was conducted by wrapping the specimens with aluminum foil (Aluminum-foil, Klinpak, Indonesia), then resting at 23°C for half a day. After 12 h, the specimens were dried in an oven at 65°C for 12 h, followed by drying at 103 ± 2°C until a steady mass was obtained.

2.2.5. Evaluation of the Physical Properties

The sengon wood characteristics were carried out through several parameters, such as weight percentage gain, anti-swelling efficiency, bulking effect, and density.

2.2.5.1. Weight percentage gain (WPG)

Impregnated sengon wood specimens were measured digitally and compared to sengon wood samples before being impregnated. The WPG was determined using Equation 1.

$$WPG\ (\%) = \frac{W1-W0}{W0} \times 100\% \quad (1)$$

where W_0 is the oven-dried weight of the sample before impregnation treatment (g), and W_1 is the oven-dried weight of the sample after impregnation treatment (g).

2.2.5.2. Anti-swelling efficiency (ASE)

ASE was evaluated by immersing the impregnated samples in the water at room temperature for 24 h (Rahayu et al. 2022). The samples were dried in an oven at 103 ± 2°C until a steady mass was obtained. ASE was determined using Equation 2.

$$ASE\ (\%) = \frac{Su-St}{Su} \times 100\% \quad (2)$$

where *Su* is the volume shrinkage of the untreated sample after being immersed for 24 h, and *St* is the volume shrinkage of the treated sample.

2.2.5.3. Bulking Effect (BE)

BE was determined using Equation 3 (Rahayu et al. 2022).

$$BE\ (\%) = \frac{V1-V0}{V0} \times 100\% \quad (3)$$

where V_0 is the oven-dried volume of the sample before impregnation treatment (cm^3), and V_1 is the oven-dried volume of the sample after impregnation treatment (cm^3).

2.2.5.4. Density (ρ)

Density was evaluated by measuring the weight and volume of the sample and calculated using Equation 4.

$$\rho\ (g/cm^3) = \frac{W1}{V1} \quad (4)$$

where W_1 is the oven-dried weight of the sample after impregnation treatment (g), and V_1 is the oven-dried volume of the sample after impregnation treatment (cm^3).

2.2.6. Evaluation of magnetic wood characteristics

The sengon magnetic wood characteristics were carried out through several parameters, such as SEM-EDS, FTIR, XRD, and VSM.

2.2.6.1. Scanning electron microscopy (SEM) and energy-dispersive X-ray spectroscopy (EDX)

The diverse morphological structures of wood and its form of cell membranes have benefited from scanning electron microscopy (SEM). Using SEM (ZEISS EVO10 series, Carl Zeiss NTS, Germany), the distribution and deposit of Fe_3O_4 nanoparticles in wooden cell membrane was examined. The treated and untreated wood samples were shaped into a cube with a side length of 0.5 cm on the tangential direction, located on an adhesive conductor, covered using conductive materials such as gold (Au), and inspected using the SEM with a 20 kV electromotive force. EDX (ZEISS SmartEDX, Carl Zeiss NTS, Germany) was employed to analyze the wood samples under 129 eV energy resolution and 1-5 nA probe current to determine the wood chemical content.

2.2.6.2. Fourier transform infrared spectrometry (FTIR) analysis

This analysis was used to detect the formation of functional groups of the material. Both untreated and impregnated wood samples were crushed into 100-mesh particles and then encapsulated in potassium bromide pellets. The final pellets were then evaluated using FTIR (Perkin-Elmer Spectrum One, PerkinElmer, USA) and scanned for 32 scans with a resolution of 4 cm^{-1} in the wavenumber range of 4.000-400 cm^{-1}.

2.2.6.3. X-ray diffraction (XRD) analysis

Sengon magnetic wood was examined utilizing an XRD (PANalytical AERIS, Malvern Panalytical, UK) apparatus with a 1D PIXcel sensor to determine the magnetic peaks and level of crystallinity. On the tangential direction, untreated and impregnated wood samples were sliced into 1-mm-thick pieces. Cu Kα radiation with a graphite monochromator, a 40 kV electric potential, a current of 30 mA, and a 2°/min scanning speed were the parameters employed in the tool. For the degree of crystallinity, the scan range was between 5 and 80 degrees. Alongside the phase analysis, it was between 5 and 90 degrees.

The XRD diffractogram and the Scherrer equation determined the average crystal size of 1% and 5% magnetite nanoparticle treatments (Lin and Ho 2014).

$$D = \frac{K\lambda}{\beta \cos\theta} \quad (5)$$

where λ represents the X-ray wavelength (0.15418 nm), K represents the Scherrer constant (0.89), β represents the peak full width at half maximum (FWHM), and θ represents the Bragg diffraction angle (Dong et al. 2015).

2.2.6.4. Vibrating sample magnetometry (VSM) analysis

The magnetic characteristics of impregnated sengon wood were detected with VSM250 (VSM Dexing Type 250, Xiamen, China) at 298-773 K outside the magnetic field from 100 Oe-21 kOe. Furthermore, the hysteresis curve was used to assess the saturation magnetization (M_S), coercivity (H_C), and remanence (M_r). The untreated and impregnated wood samples were shaped to a dimension of 3.5 mm × 3.5 mm × 1 mm on the direction of the length of the wood.

2.3. Data Analysis

A completely random design was adopted in this study, and the interactions of the concentration factor (untreated, 1%, and 5% magnetite nanoparticles) and physical properties were evaluated using ANOVA, followed by Duncan's post-hoc test at a 5% accuracy level. The IBM SPSS Statistics computer software (Version 25, SPSS Inc., USA) was implemented for all data analysis.

3. Results and Discussion

3.1. Physical Properties

3.1.1. Weight percentage gain (WPG)

WPG is one of the dimensional stability parameters, which is characterized by the addition of weight to the sample expressed in percent. The greater the percentage of WPG, the more polymer can disperse and penetrate the wood. The WPG increased as the magnetite (Fe_3O_4) nanoparticle concentration increased (**Fig. 1**). It indicates that impregnation solutions entered the test sample. The highest WPG value was obtained in the samples treated with Fe_3O_4 5% impregnation (**Fig. 1**).

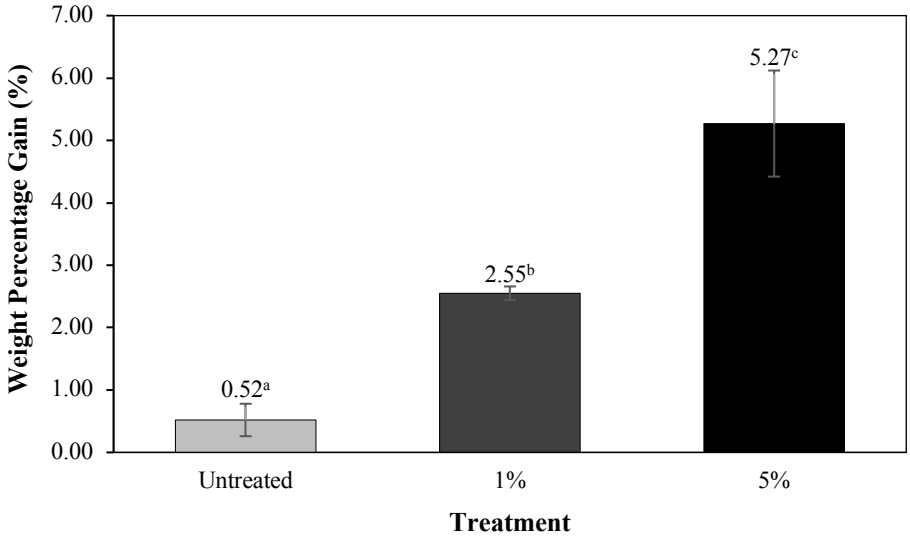

Fig. 1. Weight percentage gain of magnetic wood with different treatments.

The addition of 5% magnetite nanoparticles has a profound impact on increasing the WPG value, strengthened by the analysis of variance that showed the treatment of dispersant and concentration of magnetite nanoparticles significantly affected the WPG value. WPG value increased due to the magnetite nanoparticles that filled all the wood cavities, resulting in a rise in the total mass of the wood (Marques et al. 2005). It is slightly different from the study by Dong et al. (2015), which showed that the WPG value of magnetic wood was 27.93% because it was made with *in-situ* magnetite nanoparticles. It is caused by the formation place of *in-situ* and *ex-situ* methods. The *In-situ* method means that Fe_3O_4 nanoparticles formed inside the cavity of the wood cells, different from the *ex-situ* methods that synthesized first until it becomes nano magnetite and then applied to the wood.

3.1.2. Anti-swelling efficiency (ASE)

Wood dimensional stability values are reported as a percentage of volumetric swelling or anti-swelling efficiency (ASE). The ease of wood absorbing water affects its dimensional stability. The wood tissue will maintain a balance of moisture content with its environment through water absorption and release (Nandika et al. 1996). **Fig. 2** shows that the 5% (70.11%) magnetite nanoparticle treatment tends to be more stable than the other treatments. It might be due to the magnetite nanoparticle bulking agent, which has filled the wood and will restrain the development of the wood after soaking.

The ASE value of untreated and 1% magnetite nanoparticles was considerably different from the 5% magnetite nanoparticles because the synthesized Fe_3O_4 nanoparticles were insoluble in water. However, the nanosize could increase the solubility of magnetite nanoparticles, so agglomeration often occurs, causing the particle size to increase and making it difficult for the bulking agent to disperse into the wood cell cavities, resulting in the decrease of ASE. The low ASE is caused by the leaching of dispersants and magnetite nanoparticles due to immersion. The results show that the addition of 5% magnetite nanoparticles has a substantial influence on increasing the ASE (**Fig. 2**).

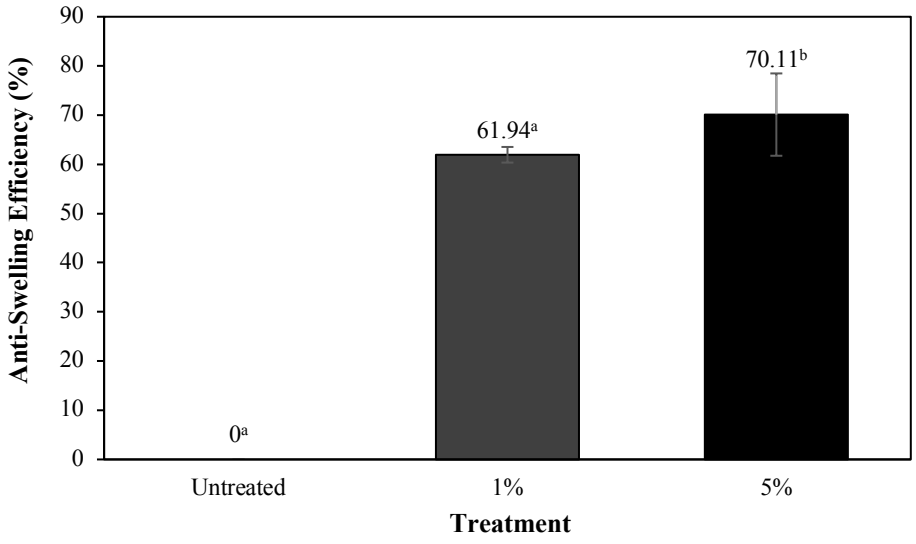

Fig. 2. ASE of magnetic wood with different treatments.

The results differed from those of Ismail (2022), who impregnated the jabon wood using NaOH precursor, showing higher results (58.17%). It was caused by the strong base precursor

having smaller particle sizes than NH_4OH, which is believed to be due to the presence of sodium metal residues and its strong alkaline properties. Consequently, when mixed with magnetite, it can reduce magnetic strength and crystallinity. However, its strong alkaline properties lead to a higher rate of magnetite core formation (Peternele et al. 2014). Despite being larger in size, NH_4OH precursor exhibits more consistency in the size distribution. Thus, it is more evenly distributed within the wood cavities.

Putri et al. (2023) stated that wood thickness swelling depends on the amount of water absorbed. The amount of absorbed water increases as the thickness expansion value increases. This study evaluated the anti-swelling efficiency because it calculates the change in volumetric swelling before and after impregnation with magnetite nanoparticles. The higher the ASE value, the more stable the dimensions of sengon wood when immersed in water. Sengon wood becomes more hydrophobic due to the bulking of magnetite nanoparticles that fill the cell lumen or bonds that occur between Fe_3O_4 and cell wall polymers during the polymerization process.

3.1.3. Bulking effect (BE)

The addition of a bulking agent can increase the wood's dimensional stability after being impregnated. **Fig. 3** shows that magnetite nanoparticles with a concentration of 5% (11.06%) gave a high BE value compared to other treatments. The BE value is directly proportional to the WPG value, showing that with an increase in WPG (**Fig. 1**), the BE also increases (**Fig. 3**).

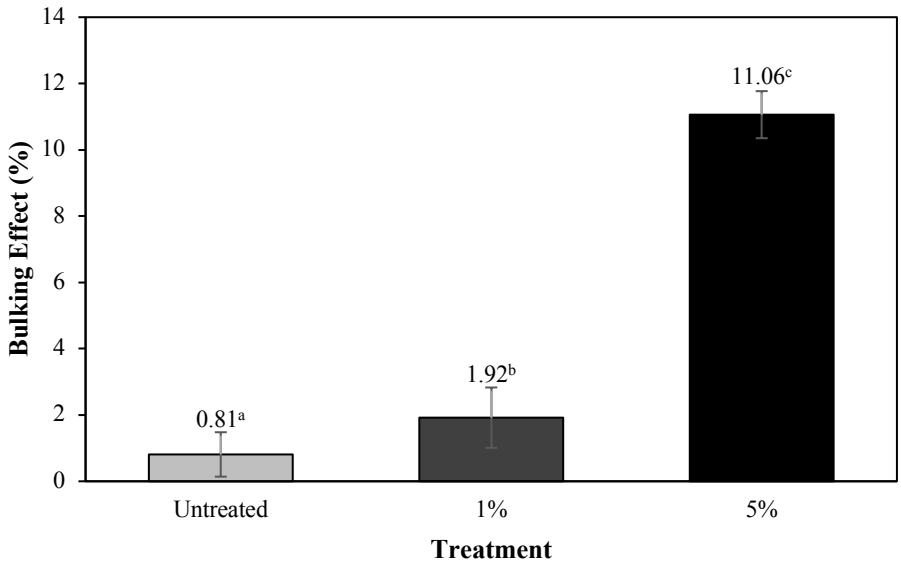

Fig. 3. BE of magnetic wood with different treatments.

The BE value of sengon wood without treatment significantly differed from the 1% and 5% concentration treatments. This shows that the addition of 5% magnetite nanoparticles has a significant effect on increasing the value of BE. After being impregnated with magnetite nanoparticles, sengon wood experienced an increase in weight linear with the increasing value of WPG. Prihatini et al. (2023) explained that magnetic wood's BE is represented by the growth in WPG, which is directionally correlated with the increase in test material dimensions. BE is one of the characteristics that identify the bulking action addition. Bulking agents are filling substances that can deposit and cover wood voids while reducing the amount of water the wood absorbs. Therefore, the dimensional stability of wood tends to rise (Syahidah and Cahyono 2008). This

result indicates that magnetite nanoparticles have the properties of a bulking agent, causing the BE value to increase. The higher the concentration of bulking agents that adhere to the wood cell walls, the higher the wood's dimensional stability, which can reduce water absorption (Hill 2006).

3.1.4. Density

Fig. 4 shows that the density increased significantly from 1% to 5% magnetite nanoparticle concentration. This result showed that the addition of magnetite nanoparticles into wood results in a denser wood structure. The 1% treated wood was not significantly different from the sample concentration of 5%. This tendency showed that the bulking mechanism of the bulking agent is less capable of dispersing the wood cell cavities because the 1% treatment particle size is lower than 20 nm. The expected standardization of nanoparticles is between 20-50 nm, as particles smaller than 20 nm tend to lose their magnetic properties (Susanti 2014).

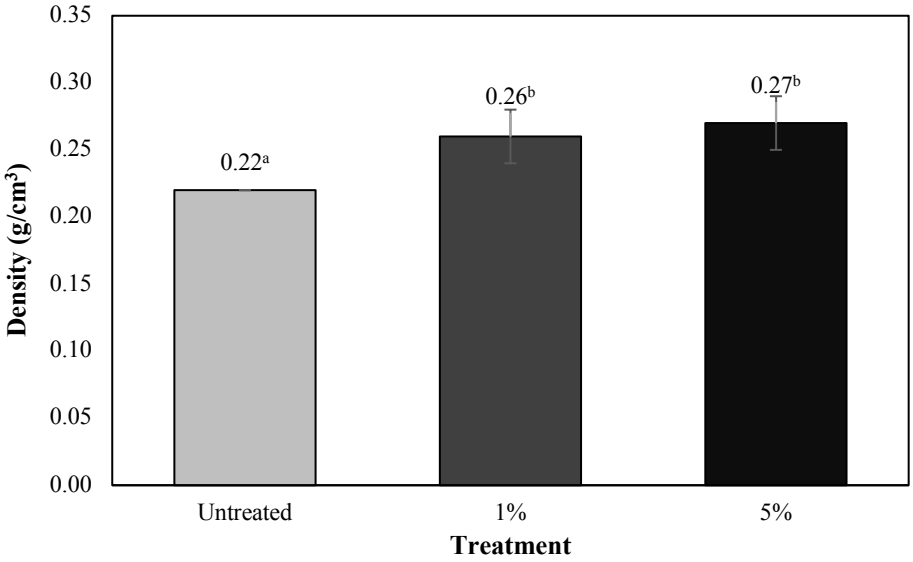

Fig. 4. Density of magnetic wood with different treatments.

The density values were slightly higher than those obtained by Moya et al. (2022) for *V. ferruginea* of 0.20 g/m^3. The difference in density is usually influenced by variations in anatomy, moisture content, and the ratio of sapwood and heartwood. Xu et al. (2019) reported that the *in-situ* method Fe_3O_4 as wood aerogel resulted in a density value of around 0.15-0.2 g/cm^3. *In-situ* formation of magnetite nanoparticles within the wood does not significantly increase the density of the wood compared to *ex-situ* formation. This value impregnated using 5% magnetite nanoparticles had a higher density than other treatments. This is because the relationship between the density value, WPG, and BE levels is straightforward. The wood density level increases as the WPG and BE levels increase.

3.2. Magnetic Properties

3.2.1. Scanning electron microscope (SEM) and energy dispersive spectrometry (EDX)

The morphology of treated and untreated wood determined using SEM are shown in **Fig. 5**. It can be seen that there are many differences in the tangential direction condition. Untreated wood shows no magnetite nanoparticles deposited on the structure (**Fig. 5a**). Sengon wood impregnated with 1% Fe_3O_4 shows that the cell cavities were evenly filled by Fe_3O_4 marked by yellowish-green

color (**Fig. 5b**). Wahyuningtyas et al. (2022) stated that the magnetite nanoparticle formation could not penetrate the wood lumen cells and instead aggregated, reducing the high surface energy of Fe_3O_4 nanoparticles. In 5% magnetic wood, there were many cracks that began to occur caused by the deposits of magnetite nanoparticles shown by the arrow (**Fig. 5c**). However, the deposits of Fe_3O_4 in the cavity are more than a concentration of 1%. This happens because the 5% solution was thicker than 1%, making the impregnation solution that has entered the cell cavity more difficult to penetrate. However, the cell cavity holds more of it, so it is less likely that the impregnant will come out of the cell cavity. Moya et al. (2022) found that the occurrence of Fe_3O_4 in such anatomical components is anticipated. Hardwood species' fibers serve as structural elements rather than liquid transport vessels. Therefore, there is a low expectation of *ex-situ* formation of Fe_3O_4 in the fibers.

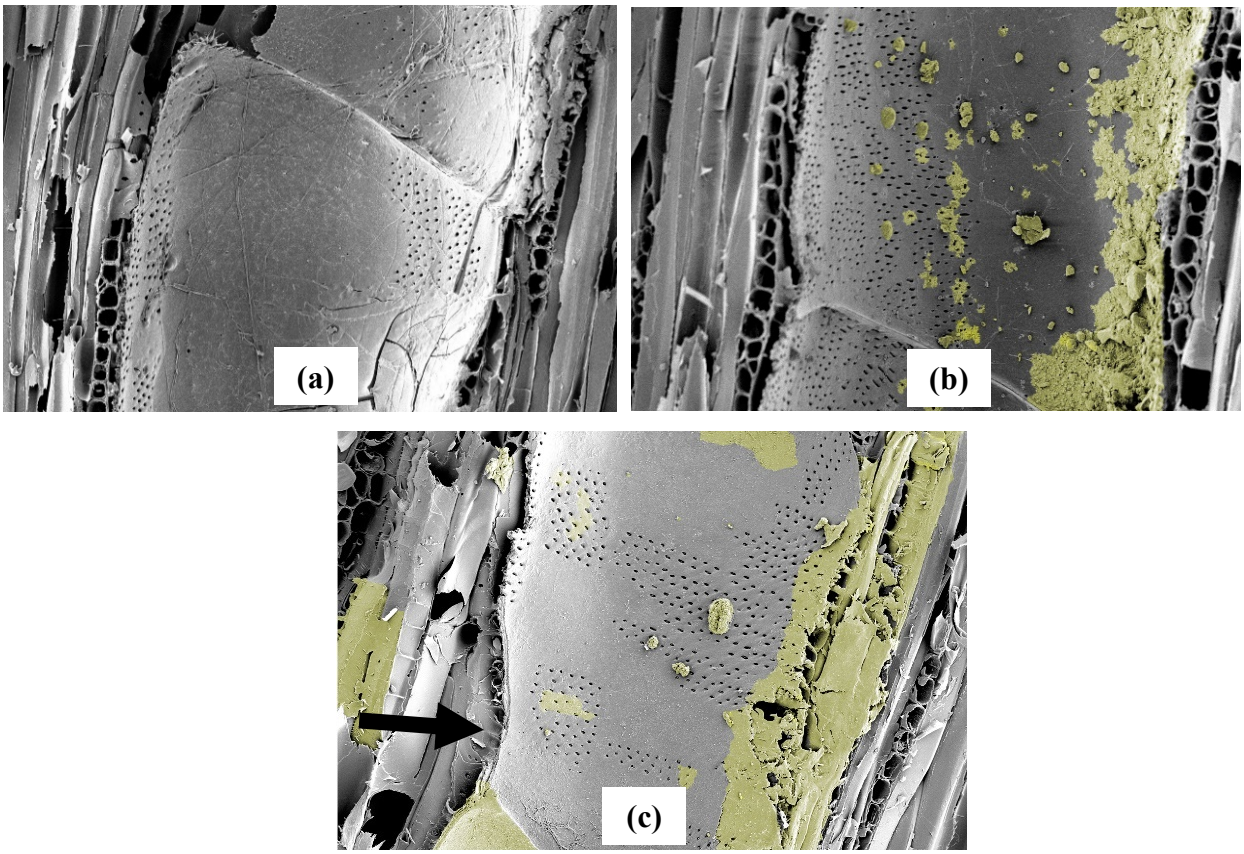

Fig. 5. SEM analysis results: (a) untreated, (b) Fe_3O_4 1%, (c) Fe_3O_4 5%.

Moreover, an elemental analysis method connected to electron microscopy is called EDX microanalysis, which reveals the inorganic chemical composition of the cell wall and various inclusions. The occurrence of Fe_3O_4 through EDX analysis proved that it was inside the wood cavity, and the outcomes are displayed in **Table 2**.

Table 2. Chemical composition of impregnated sengon wood with different treatments

Wood sample	C (wt%)	O (wt%)	Fe (wt%)
Untreated	55.3 ± 0.4	44.7 ± 0.4	0.00
Fe_3O_4 1%	53.3 ± 1.3	46.7 ± 1.3	3.47 ± 0.5
Fe_3O_4 5%	52.1 ± 0.5	47.2 ± 0.5	5.43 ± 0.9

The proportion of magnetite nanoparticles (Fe_3O_4 nanoparticles) in untreated wood increased from 1% to 5% (**Table 2**). Xue and Zhao (2008) stated that nanoparticles could infiltrate and penetrate wood, particularly through nanosized cavities. Based on research by Irianti et al. (2021), the morphology of Fe_3O_4 synthesized with demineralized water appeared to be agglomerated. As a result, the particles find it more challenging to enter the wood cells due to their relatively large size (further explained in the XRD analysis). Another study by Mohamed et al. (2017) stated that the elemental composition of Fe at bulk Fe_3O_4 nanoparticles was about 37.20%, higher than this study because that was before impregnated to the wood.

3.2.2. Fourier transform infrared spectrometry (FTIR) analysis

Fig. 6 displays the absorption bands for the O-H stretching vibration of hydroxyl groups of untreated wood at 3336 cm^{-1}, then shifting into 3335 cm^{-1} and 3339 cm^{-1} for Fe_3O_4 1% and 5%. Hazarika and Maji (2014) revealed O-H bending at a wavenumber of 3340 cm^{-1} in the cell membrane material, while Nandiyanto et al. (2019) stated that hydroxyl group's bending radius falls between 3570 cm^{-1} and 3200 cm^{-1}. In addition, a peak at 3400 cm^{-1} shows a molecular structure of water in the liquid phase (Cheng et al. 2013).

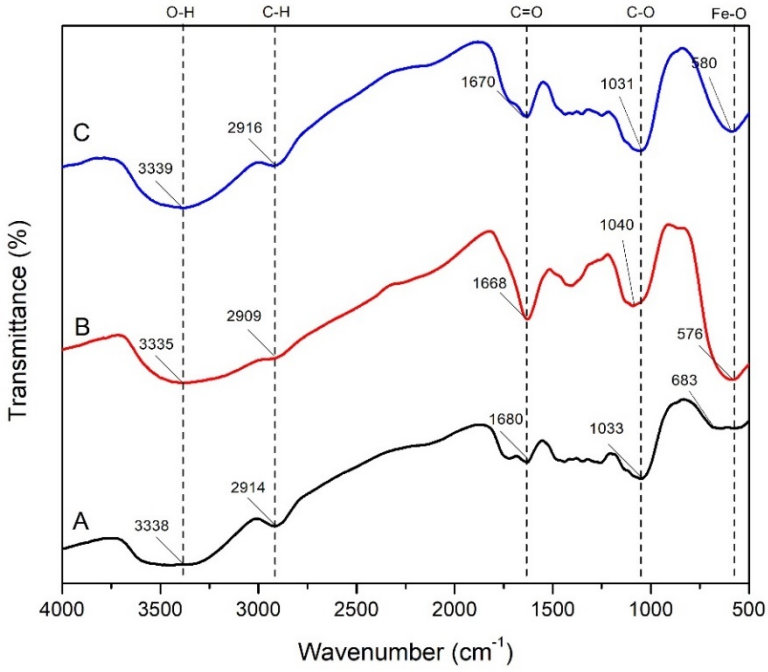

Fig. 6. FTIR analysis results: (a) untreated, (b) Fe_3O_4 1%, (c) Fe_3O_4 5%.

There is a new absorption band at a wavenumber of 2906 cm^{-1}. The detected peak vibrations ranged from 2909 cm^{-1} for Fe_3O_4 1%, then shifting to 2914 and 2916 cm^{-1} for untreated and Fe_3O_4 5%. Therefore, Earlier studies by Gan et al. (2017) linked the existence of an asymmetrical C-H functional group at a wavenumber of 2908 cm^{-1} with the tremors of the C-H stretching functional group, and this peak demonstrated the presence of that group. It was seen that C=O is the functional group resonance at 168–1670 cm^{-1} wavenumber. Based on Larkin (2017), the detected peak with an absorption wavenumber of 1685-1666 cm^{-1} showed the group of C=O intensified hemicelluloses. The cellulose's structure is represented by a wavenumber of 1040 cm^{-1}, confirming cellulose's C-O contraction vibrations (Hazarika and Maji 2014). Another absorption with a wavenumber of 576 cm^{-1} confirms the appearance of the Fe-O functional groups, then shifted to

580 cm^{-1} in the 5% treatment. This finding indicates that Fe_3O_4 was deposited on the wood substrate. The untreated wood absorbs at the wavenumber of 663 cm^{-1}, indicating no Fe-O group in this sengon wood. It is straightened out by Mohamed et al. (2017) that due to the vibrations of Fe_3O_4, Fe-O absorption peaks are concentrated at 557 cm^{-1}.

3.2.3. X-ray diffraction (XRD) analysis

Fig. 7 shows the XRD patterns of the untreated and impregnated sengon wood. It was observed that there are two physical phases due to the presence of cellulose that has crystal planes (021) and peaks at 2θ values of 23.37° and 22.92°. The graph showed that the higher the concentration, the graph becomes flatter. According to Rahayu et al. (2021), the crystalline cellulose area in sengon wood has changed to amorphous.

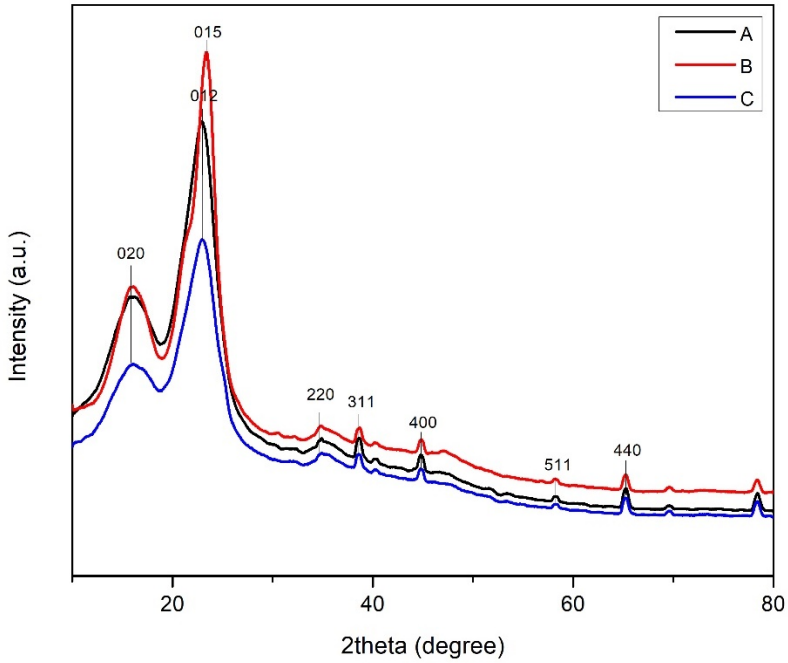

Fig. 7. Results of the XRD research on Sengon wood: (a) untreated, (b) Fe_3O_4 1%, (c) Fe_3O_4 5%.

Additional peaks were produced after the Fe_3O_4 treatment at 1%, showing that magnetite compounds had formed in the wood that take place at a value of 2θ 38.60° with the crystal plane (311), values of 2θ 43.00°, 42.82°, and 43.10° with the crystal plane (400), value of 2θ 44.83° with the crystal plane (400), value of 2θ 58.27° with the crystal plane (511), and value of 2θ 62.24° for untreated wood and 62.17° for impregnated wood with the crystal plane (440) (Wu et al. 2011). Fe_3O_4 peaks occur at approximately 23.37.1°, 38.60°, 43.1°, 44.83°, 58.27°, and 62.24°. A comparison study showed that the materials' peaks displayed the magnetite spinel's predominant phase of the powdered cubic crystal structure. The resulting particles were primarily pure Fe_3O_4 in contrast to the bulk magnetite from Daoush (2017), and the structure was a face-centered cubic crystal structure. The outcome is consistent with the observations made by Dong et al. (2015) and Rahayu et al. (2022), who demonstrated the existence of magnetite compounds at these peaks. Following the treatment, due to the availability of all diffraction peaks connected to both wood and Fe_3O_4 in the magnetic wood, the magnetic Fe_3O_4 particles have been effectively placed over the wooden substrate (Gan et al. 2017).

The size of the Fe_3O_4 particles in wood sample with 1% treatment was smaller than the 5% treatment (**Table 3**). In contrast, the degree of crystallinity tends to decrease with the increase of Fe_3O_4 (**Table 3**). The 5% magnetite nanoparticles treatment exhibits a stronger presence of magnetite. Khan et al. (2018) defined something as nanosized if its size is between 1 and 100 nm. Particle size, crystal size, and surface area are the most significant physical characteristics of materials that influence solubility (Cornell and Schwertmann 2006). Due to the presence of several quasicrystalline regions in hemicellulose and cellulose, which cause wood to crystallize (Bhuiyan et al. 2000), the physical phases caused by the presence of cellulose were weakened after processing. The last peak may be hidden by other peaks, showing that the magnetization may have destroyed a portion of the wood's crystal structure (Dong et al. 2014). Daoush (2017) reported nanoparticles of approximately 30 nm in size, as a result of the production of a monolayer covering of magnetite in the presence of EDTA. The result was less agglomerated, demonstrating the feasibility of synthesizing homogeneous magnetite nanoparticles. The results of the current study are excellent than the previous publications that employed the co-precipitation approach.

Table 3. Crystallinity level of untreated and impregnated sengon wood with Fe_3O_4 nanoparticles

Wood sample	Degree of crystallinity (%)	Size of Fe_3O_4 particles (nm)
Untreated	46.23	-
Fe_3O_4 1%	46.28	19.30
Fe_3O_4 5%	40.64	33.63

3.2.4. Vibrating sample magnetometry (VSM) analysis

VSM is utilized to measure the magnetic characteristics of magnetic materials. The materials to be studied are subjected to persistent magnetism (Kirupakar et al. 2016). The magnetization curve, known as the hysteresis loop, results from the VSM study of impregnated sengon wood. **Fig. 8** depicts the sengon wood's magnetic hysteresis peaks that have been impregnated and untreated. When an object comes into contact with a magnetic field from the outside and when the magnetic field is gone, the opposite current is also present on the hysteresis curve that is virtually aligned (Tebriani 2019).

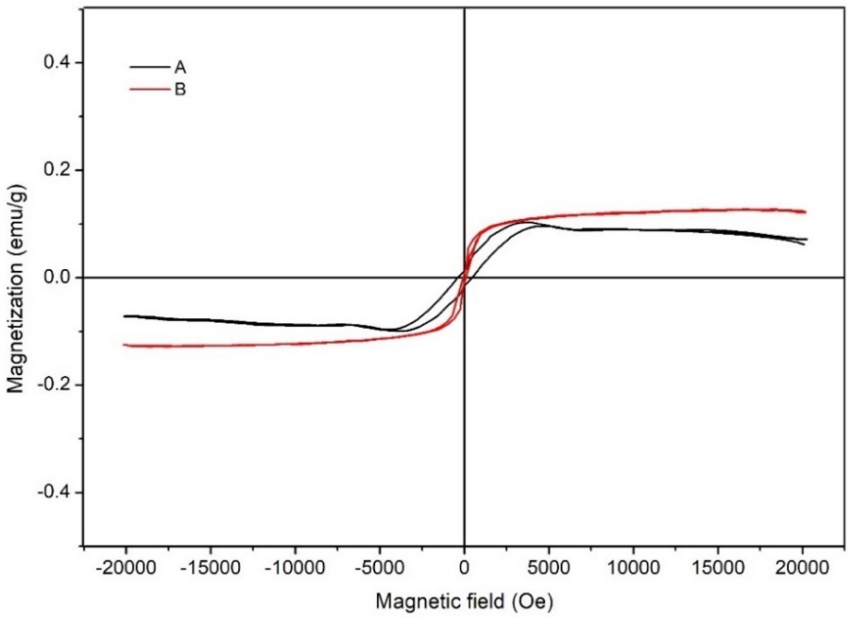

Fig. 8. VSM analysis results of sengon wood: (a) Fe_3O_4 1%, (b) Fe_3O_4 5%.

The size of the hysteresis curve reveals the amount of energy needed to magnetize the materials. By saturation magnetization (M_S), remanence (M_r), and coercivity (H_C), VSM produces a hysteresis curve. Fe_3O_4 5% nanoparticles show a higher M_S value than 1% nanoparticles (**Table 4**). The M_r values for the treatments consecutively are 0.012 and 0.014. The M_r values in this investigation were higher than those reported by Moya et al. (2022) and Rahayu et al. (2022), who reported M_r values of 0.01 emu/g and 0.01 to 0.25 emu/g, respectively. The magnetite crystal size in this research was bigger than Rahayu et al. (2022), which was 10.1996 nm for the weak base. Mohamed et al. (2017) previously studied the VSM behavior of Fe_3O_4 before and after blending with other components, resulting in identical actions at the hysteresis.

Table 4. The saturation magnetization (M_S), coercivity (H_C), and remanence (M_r) of the impregnated sengon wood

Treatment	M_S (emu/g)	M_r (emu/g)	H_C (Oe)
1%	0.06	0.012	1.18×10^{-4}
5%	0.12	0.014	1.85×10^{-4}

The H_C values for Fe3O4 1% and 5% were 1.18×10^{-4} Oe and 1.85×10^{-4} Oe, respectively. The low coercivity field value was assigned to the impregnated wood H_C value. Given that the H_C value is tiny or close to zero and that the curve representing the hysteresis region normally has a flat and thin shape, this might be viewed as low. The H_C value approaching zero raises the possibility that the magnetic sengon wood has superparamagnetic characteristics (Hui et al. 2008; Rahayu et al. 2022; Xu et al. 2005). The term "soft magnetic materials" can be used to describe magnetic sengon wood (Karbeka et al. 2020; Marta et al. 2020; Widanarto et al. 2018). The magnetic intensity quickly returns to zero when the external magnetic field is withdrawn, and soft magnetic characteristics are easily magnetized and affected by the external magnetic field (Wicaksono et al. 2018).

Fig. 9 displays the relationship between the WPG and M_S. The M_S value is linear to the WPG value, according to Gao et al. (2012), who are the authors of this study. The Ms value also dropped along with the WPG value. According to Riyanto (2012), the degree of crystallinity and the size of the nanoparticles' grains are two examples of the many variables that may contribute to variations in saturation magnetization levels. These results strengthened with another study, but it is slightly different from Laksono et al. (2023), who stated that the particle size of the magnetite nanoparticles was 31.72 nm. The difference can be attributed to the type of magnetite nanoparticles. Because sengon wood is fast-growing, it is still dominated by juvenile wood. In other literature, Oka et al. (2002) stated that sapwood could receive more magnetic fluid than heartwood because of the long fibers.

Based on Chicco et al. (2021), the graph displayed the observable adjusted for the correlation coefficient, which is near 1. Rahayu et al. (2022) and Dong et al. (2015) reported similar results that the WPG value is directly proportional to the M_S value. Kirupakar et al. (2016) stated that the higher the magnetization, the higher the induced current because this correlation shows that the magnetite nanoparticles could be well distributed. This case might have resulted from the impact of impregnated sengon wood being different from bulk magnetite nanoparticles. It decreases the wood's crystallinity, resulting in a lower M_S value in this research than in bulk magnetite nanoparticles (Gan et al. 2017).

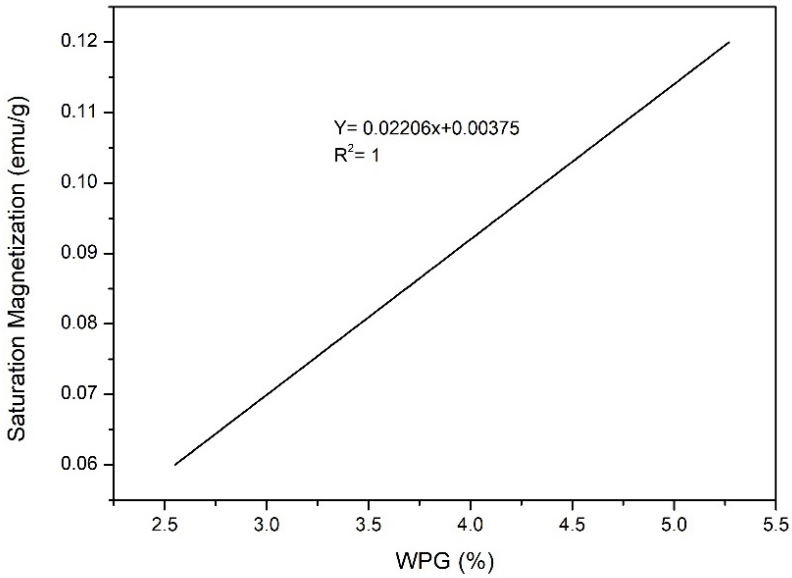

Fig. 9. The correlation between magnetic sengon wood's saturation magnetization (Ms) and weight percentage gain (WPG).

4. Conclusions

Sengon wood impregnation with magnetite nanoparticles significantly improved the density and dimensional stability of the wood, as indicated by the increase in weight percentage gain, anti-swelling efficiency, and bulking effect. Characterization test results showed promising outcomes, showing changes in the sengon wood's morphology due to the presence of Fe that deposited and covered the cell membranes of wood. The impregnated wood contained Fe-O functional groups and a higher degree of crystallinity than untreated wood. The impregnated sengon wood with Fe_3O_4 nanoparticles is classified as soft magnetic with superparamagnetic properties. According to the VSM investigation, the impregnated wood has stronger magnetic properties than untreated wood, demonstrated by a higher M_S value.

Acknowledgments

This research was funded by The Directorate of Higher Education, Research and Technology of the Ministry of Education, Culture, Research and Technology of the Republic of Indonesia with the Postgraduate-Research-Master-Thesis Research scheme (PPS-PTM) (Contact Number 102/E5/PG.02.00.PL/2023 and 18905/IT3.D10/PT.01.02/M/T/2023).

References

Bhuiyan, M.T.R., Hirai, N., and Sobue, N. 2000. Changes of Crystallinity in Wood Cellulose by Heat Treatment Under Dried and Moist Conditions. *Journal of Wood Science* 46(6): 431–436. DOI: 10.1007/bf00765800

British Standard Institution. 1957. *BS 373:1957 – Methods of Testing Small Clear Specimens of Timber*. British Standard Institution (BS).

Cheng, F., Cao, Q., Guan, Y., Cheng, H., Wang, X., and Miller, J. D. 2013. FTIR Analysis of Water Structure and Its Influence on The Flotation of Arcanite (K_2SO_4) and Epsomite ($MgSO_4 \cdot 7H_2O$). *International Journal of Mineral Processing* 122: 36–42. DOI: 10.1016/j.minpro.2013.04.007

Chicco, D., Warrens, M. J., and Jurman, G. 2021. The Coefficient of Determination R-squared is More Informative Than SMAPE, MAE, MAPE, MSE and RMSE in Regression Analysis Evaluation. *PeerJ Computer Science* 7: 1–24. DOI: 10.7717/peerj-cs.623

Cornell, R.M., Schwertmann U. 2006. *The Iron Oxides: Structure, Properties, Reactions, Occurrences and Ues*. John Wiley and Sons, New York, NY, USA.

Daoush, W. M. 2017. Co-precipitation and Magnetic Properties of Magnetite Nanoparticles of Potential Biomedical Applications. *Journal of Nanomedicine Research* 5(3): 1–6. DOI: 10.15406/jnmr.2017.05.00118

Dong, Y., Yan, Y., Zhang, S., Li, J. 2014. Wood/polymer Nanocomposites Prepared by Impregnation with Furfuryl Alcohol and Nano SiO_2. *BioResources* 9(4): 6028–6040. DOI: 10.15376/biores.9.4.6028-6040

Dong, Y., Yan, Y., Zhang, Y., Zhang, S., and Li, J. 2015. Combined Treatment for Conversion of Fast-Growing Poplar Wood to Magnetic Wood with High Dimensional Stability. *Wood Science and Technology* 50(3): 503–517. DOI: 10.1007/s00226-015-0789-6

Fajriani, E., Ruelle, J., Dlouha, J., Fournier, M., Hadi, Y. S., and Darmawan, I. W. 2013. Radial Variation of Wood Properties of Sengon (*Paraserianthes falcataria*) and Jabon (*Anthocephalus cadamba*). *Journal of Indian Academy of Wood Science* 10(2): 110–117. DOI: 10.1007/s13196-013-0101-z

Fufa, S. M., and Hovde, P. J. 2010. Nano-Based Modifications of Wood and Their Environmental Impact: Review. *11th World Conference on Timber Engineering 2010, WCTE 2010* 3(1): 2387–2388.

Gan, W., Gao, L., Xiao, S., Gao, R., Zhang, W., Li, J., and Zhan, X. 2017. Magnetic Wood as an Effective Induction Heating Material: Magnetocaloric Effect and Thermal Insulation. *Advanced Materials Interfaces* 4(22): 1–9. DOI: 10.1002/admi.201700777

Gao, H. L., Wu, G. Y., Guan, H. T., and Zhang, G. L. 2012. *In Situ* Preparation and Magnetic Properties of Fe_3O_4/ Wood Composite. *Materials Technology* 27(1): 101–103. DOI: 10.1179/175355511x13240279339806

Hazarika, A., and Maji, T. K. 2014. Modification of Softwood by Monomers and Nanofillers. *Defence Science Journal* 64(3): 262–272. DOI: 10.14429/dsj.64.7325

Hill, C. A. S. 2006. *Wood Modification: Chemical, Thermal, and Other Processes*. John Wiley and Sons Ltd, West Sussex. DOI: 10.1002/0470021748

Hui, C., Shen, C., Yang, T., Bao, L., Tian, J., Ding, H., Li, C., and Gao, H. J. 2008. Large-Scale Fe_3O_4 Nanoparticles Soluble in Water Synthesized by A Facile Method. *The Journal of Physical Chemistry* 112(30): 11336–11339. DOI: 10.1021/jp801632p

Irianti, F. D. D., Sutanto, H., Wibowo, A. A., Syahida, A. N., and Alkian, I. 2020. Characterization Structure of Fe3O4@PEG-4000 Nanoparticles Synthesized by Co-precipitation Method. *Journal of Physics: Conference Series* 1943(2021): 1–8. DOI: 10.1088/1742-6596/1943/1/012014.

Ismail, R. 2022. *Karakteristik Kayu Jabon (Anthocephalus cadamba) Terimpregnasi Partikel Nano Magnetit* (Fe_3O_4). Universitas Nusa Bangsa, Bogor.

Karbeka, M., Koly, F. V. L., and Tellu, N. M. 2020. Characterization of the Magnetic Properties of Iron Sand Puntaru Beach, Alor – NTT Regency. *Lantanida Journal* 8(2): 96–188. DOI: 10.22373/lj.v8i2.7867

Khan, S. A., Khan, L. U., and Asiri, A. M. 2018. *Fourier Transform Infrared Spectroscopy: Fundamentals and Applications in Functional Groups and Nanomaterials Characterization*. University of Swabi, Pakistan. DOI: 10.1007/978-3-319-92955-2_9

Kirupakar, B. R., Vishwanath, B. A., and Sree, M. P., Deenadayalan. 2016. Vibrating Sample Magnetometer and Its Application in Characterisation of Magnetic Property of the Anti-Cancer Drug Magnetic Microspheres. *International Journal of Pharmaceutics and Drug Analysis* 4(5): 227–233.

Krisnawati, H., Varis, E., Kallio, M., and Kanninen, M. 2011. *Paraserienthes falcataria* (L.) Nielsen*: Ekologi, Silvikultur dan Produktivitas*. CIFOR, Bogor.

Laksono, G. D., Rahayu, I. S., Karlinasari, L., Darmawan, W., and Prihatini, E. 2023. Characteristics of Magnetic Sengon Wood Impregnated with Nano Fe_3O_4 and Furfuryl Alcohol. *Journal of the Korean Wood Science and Technology* 51(1): 1–13. DOI: 10.5658/wood.2023.51.1.1

Larkin, P. 2017. *Infrared and Raman Spectroscopy: Principles and Spectral Interpretation.* Elsevier Science, Netherlands.

Lin, C. C., and Ho, J. M. 2014. Structural Analysis and Catalytic Activity of Fe_3O_4 Nanoparticles Prepared by A Facile Co-Precipitation Method in A Rotating Packed Bed. *Ceramics International* 40(7): 10275–10282. DOI: 10.1016/j.ceramint.2014.02.119

Liu, T. T., Cao, M. Q., Fang, Y. S., Zhu, Y. H., and Cao, M. S. 2022. Green Building Material Lit Up by Electromagnetic Absorption Function: A Review. *Journal Material Science and Technology* 112: 329–344. DOI: 10.1016/j.jmst.2021.10.022

Marques, P. A. A. P., Trindade, T., and Neto, C. P. 2005. Titanium Dioxide/Cellulose Nanocomposites Prepared by A Controlled Hydrolysis Method. *Composites Science and Technology* 66: 1038–1044. DOI: 10.1016/j.compscitech.2005.07.029

Marta, R., Darvina, Y., Ramli, and Desnita. 2020. Effect of $MnFe_3O_4$ Composition on Magnetic Properties of $MnFe_3O_4$/PVDF Nanocomposite Prepared by Spin Coating Method. *Pillar of Physics* 13(1): 42–50. DOI: 10.24036/7870171074

Mashkour, M., and Ranjbar, Y. 2018. Superparamagnetic Fe_3O_4 @ Wood Flour/Polyprophylene Nano Composite: Physical and Mechanical Properties. *Industrial Crops and Products* 111: 47–54. DOI: 10.1016/j.indcrop.2017.09.068

Mohamed, S. A., Al-Harbi, M. H., Almulaiky, Y. Q., Ibrahim, H., and El-Shishtawy, R. M. 2017. Immobilization of Horseradish Peroxidase on Fe_3O_4 Magnetic Nanoparticles. *Electronic Journal of Biotechnology* 27:84–90.

Moya, R., Gaitan-Alvarez, J., Berrocal, A., and Merazzo, K. J. 2022. *In Situ* Synthesis of Fe_3O_4 Nanoparticles and Wood Composite Properties of Three Tropical Species. *Materials* 15(3394): 1–17. DOI: 10.3390/ma15093394

Nandika, D., Soenaryo, and Saragih, A. 1996. *Kayu dan Pengawetan Kayu*. Dinas Kehutanan DKI, Jakarta.

Nandiyanto, A. B. D., Oktiani, R., and Ragadhita, R. 2019. How to Read and Interpret FTIR Spectroscope of Organic Material. *Indonesian Journal of Science and Technology* 4(1): 97–118. DOI: 10.17509/ijost.v4il.15806

Oka, H., and Fujita, H. 1999. Experimental Study on Magnetic and Heating Characteristics of Magnetic Wood. *Journal of Applied Physics* 85(8): 5730–5734. DOI: 10.1063/1.370267

Oka, H., Hojo, A., Seki, K., and Takashiba, T. 2002. Wood Construction and Magnetic Characteristics of Impregnated Type Magnetic Wood. *Journal of Magnetism and Magnetic Materials* 239: 617–619. DOI: 10.1016/S0304-8853(01)00684-9

Peternele, W. S., Fuentes, V. M., Fascineli, M. L., da Silva, J. R., Silva, R. C., Lucci, C. M., and de Azevedo, R. B. Experimental Investigation of The Co-Precipitation Method: an Approach to Obtain Magnetite and Maghemite Nanoparticles with Improved Properties. *Journal of Nanomaterials* 2014: 1–10. DOI: 10.1155/2014/682985

Priadi T., Sholihah M., and Karlinasari L. 2019. Water Absorption and Dimensional Stability of Heat-Treated Fast-Growing Hardwoods. *Journal of the Korean Wood Science and Technology* 47(5): 567–578. DOI: 10.5658/wood.2019.47.5.567

Prihatini, E., Wahyuningtyas, I., Rahayu, I. S., and Ismail, R. 2023. The Modification of Fast-Growing Wood into the Magnetic Wood Using Fe_3O_4 Nanoparticles Impregnation. *Jurnal Sylva Lestari* 11(2): 204–217. DOI: 10.23960/jsl.v11i2.651

Putri, A. R., Alam, N., Adzkia, U., Amin, Y., Darmawan, I. W., and Karlinasari, L. 2023. Physical and Mechanical Properties of Oriented Flattened Bamboo Boards from Ater (*Gigantochloa atter)* and Betung (*Dendrocalamus asper*) bamboos. *Jurnal Sylva Lestari* 11(1): 1–21. DOI: 10.23960/jsl.v11i1.614

Rahayu, I. S., Pratama, A., Darmawan, W., Nandika, D., and Prihatini, E. 2021. Characteristics of Impregnated Wood by Nano Silica from Betung Bamboo Leaves. *IOP Conference Series: Earth and Environmental Science* 891: 12019. DOI: 10.1088/1755-1315/891/1/012019

Rahayu, I. S., Prihatini, E., Ismail, R., Darmawan, W., Karlinasari, L., and Laksono, G.D. 2022. Fast-Growing Magnetic Wood Synthesis by an *In-Situ* Method. *Polymers* 14(11): 2137. DOI: 10.3390/polym14112137

Riyanto, A. 2012. Synthesis of Fe_3O_4 Nanoparticles and Their Potential as Active Materials on Surface Sensing Biosensors Based on SPR. M.S. Thesis, Postgraduate Program, Gadjah Mada University, Indonesia.

Susanti, S. 2014. *Kajian Struktur Kristal Nanopartikel Magnetite (Fe_3O_4) Sebagai Fungsi Temperatur dari Hasil Sintesis dengan Menggunakan Metode Sonokimia.* Yogyakarta: Universitas Islam Negeri Sunan Kalijaga.

Sutopo, E. H. 2019. Proses Demineralisasi Air Tanah Menjadi Air TDS 0 PPM Menggunakan Metode Resin Penukar Ion Tunggal (Single Ionic Resin Exchange Method). *Jurnal Inovasi Ilmu Pengetahuan dan Teknologi* 1(1): 22-10. DOI: 10.32493/jiptek.v1i1.4590

Syahidah, and Cahyono, T. D. 2008. Stabilisasi Dimensi Kayu dengan Aplikasi Parafin Cair. *Perennial* 4(1): 18–22. DOI: 10.24259/perennial.v4i1.178

Tebriani, S. 2019. Analysis of the Vibrating Sample Magnetometer (VSM) on the Results of the Electrodeposition of a Thin Layer of Magnetite using a Continuous Direct Current. *Natural Science Journal* 5(1): 722–730. DOI: 10.15548/nsc.v5i1.892

Teng, T. J., Arip, M. N. M., Sudesh, K., Nemoikina, A., Jalaludin, Z., Ng, E. P., and Lee, H. L. 2018. Conventional Technology and Nanotechnology in Wood Preservation: A Review. *BioResources* 13(4): 9220–9252. DOI: 10.15376/biores.13.4.teng

Trey S. M., Olsson R. T., Strom V., Berglund L. A., and Johansson M. 2014. Controlled Deposition of Magnetic Particles Within The 3-D Template Wood: Making Use of The Natural

Hierarchical Structure of Wood. *RSC Adv*ances 4(1): 35678–35685. DOI: 10.1039/c4ra04715j

Wahyuningtyas, I., Rahayu, I. S., Maddu, A., and Prihatini, E. 2022. Magnetic Properties of Wood Treated with Nano-Magnetite and Furfuryl Alcohol Impregnation. *Bioresources* 17(4): 6496–6510. DOI: 10.15376/biores.17.4.6496-6510

Wicaksono, A., Rohman, L., and Supriyanto, E. 2018. Study of Ferromagnetic Resonance BaFe12O19 Using Micromagnetic Simulation. *Berkala Sainstek* 6(1): 46–48.

Widanarto, W., Ardenti, E., Ghosal, S. K., Kurniawan, C., Effendi, M, and Cahyanto, W. T. 2018. Significant Reduction of Saturation Magnetization and Microwave-Reflection Loss in Barium-Natural Ferrite Via Nd^{3+} Substitution. *Journal of Magnetism and Magnetic Materials* 456: 288–291. DOI: 10.1016/j.jmmm.2018.02.050

Wu, S., Sun, A., Zhai, F., Wang, J., Xu, W., Zhang, Q., and Volinsky, A.A. 2011. Fe_3O_4 Magnetic Nanoparticles Synthesis from Tailings by Ultrasonic Chemical Co-Precipitation. *Materials Letters* 65(12): 1882–1884. DOI: 10.1016/j.matlet.2011.03.065

Xu, L., Xiong, Y. Dang, B., Ye, Z., Jin, C. Sun, Q., and Yu, X. 2019. *In-Situ* Anchoring of Fe_3O_4/ZIF-67 Dodecahedrons in Highly Compressible Wood Aerogel with Excellent Microwave Absorption Properties. *Materials and Design* 182(2019): 1–9. DOI: 10.1016/j.matdes.2019.108006

Xu, Z. Z., Wang, C. C., Yang, W. L., and Fu, S.K. 2005. Synthesis of Superparamagnetic Fe_3O_4/SiO_2 Composite Particles via Sol-Gel Process Based on Inverse Mini Emulsion. *Journal of Materials Science* 40(17): 4667–4669. DOI: 10.1007/s10853-005-3924-1

Xue, F., and Zhao, G. 2008. Optimum Preparation Technology for Chinese Fir Wood/Ca-Montmorillonite (Ca-MMT) Composite Board. *Forestry Studies in China* 10(3): 199–204. DOI: 10.1007/s11632-008-0039-1

Zelinka, S. L., Altgen, M., Emmerich, L., Guigo, N., Keplinger, T., Kymalainen, M., Thybring, E. E., and Thygesen, L. G. 2022. Review of Wood Modification and Wood Functionalization Technologies. *Forests* 13(7): 1–46. DOI: 10.3390/f13071004

Zhang X., Zhou R., Rao W., Cheng Y., and Ekoko, B. G. 2006. Influence of Precipitator Agents NaOH and NH_4OH on The Preparation of Fe_3O_4 Nanoparticles Synthesized by Electron Beam Irradiation. *Journal of Radioanalytical and Nuclear Chemistry* 270: 285–289. DOI: 10.1007/s10967-006-0346-8